DOI: 10.1002/chem.200800478

Synthesis of Compounds Presenting Three and Four Anthracene Units as Potential Connectors To Mediate Infinite Lateral Growth at the Air/Water Interface

Cindy Münzenberg,[a] Antonella Rossi,[a, b] Kirill Feldman,[a] Reto Fiolka,[c] Andreas Stemmer,[c] Katarzyna Kita-Tokarczyk,[d] Wolfgang Meier,[d] Junji Sakamoto,[a] Oleg Lukin,[a] and A. Dieter Schlüter*[a]

Abstract: We report the synthesis of molecular sheets based on the photochemically initiated dimerization of monomers with lateral anthracene units. The film thickness and composition were investigated by ellipsometry and X-ray photoelectron spectroscopy (XPS). The mechanical stability of the film was sufficient to span it over 45× 45 μm-sized holes. Several model reactions were performed to illustrate the underlying chemistry and to assist in analysis. The reported experiments are considered first steps towards the ultimate goal of the rational synthesis of laterally "infinite", one-monomer-unit-thick molecular sheets with a long-range positional order and a periodic covalent-bonding pattern. Such sheets are referred to as 2D polymers and are considered a prime goal of chemical synthesis with intriguing applications.

Keywords: anthracenes · calixarenes · photodimerization · polymers · unimolecular films

Introduction

Practically all bio- and synthetic polymers known today consist of single-stranded, covalent backbones. The indispensable functions of many for both life in general and in the daily life of every human being result from their chemical structure and how these macromolecules arrange into higher-order structures. For some applications, polymers both as ultrathin film and in bulk are used in a networked form and cease to be considered as single stranded. Because the segments between the netpoints have a length distribution they cannot be regarded as ordered 2D or 3D structures either. The creation of useable, "infinitely" extended, covalently constructed and structurally defined, periodic 2D polymers has been a dream of chemists for decades and numerous attempts towards this goal have been reported.[1] A non-comprehensive list of relevant articles can be found in the literature.[2–7] Though enormous progress has been made, even today no synthetic polymer is known that meets all the above criteria.[8] The mastering of the very high level of structure control inherently associated with a realization of such a goal can be considered a major driving force for our work in this area. Also, given the structural novelty of periodic 2D polymers, the exploration of their property space is another major motivation. We have initiated projects aiming at achieving the above goal and wish to disclose some initial steps here. These steps are based on amphiphilic monomers capable of forming stable Langmuir monolayers at the air/water interface and of undergoing subsequent polymerization in the compressed state. The monomers presented here are based on three-armed branched molecules of kind **A** and calixarenes of kind **B** (Figure 1) with three and four pendent anthracenes, respectively. They are designed so as to exploit the well-studied photochemically induced anthracene dimerization[9] as the key reaction ideally resulting in

[a] Dipl.-Chem. C. Münzenberg, Prof. Dr. A. Rossi, Dr. K. Feldman, Dr. J. Sakamoto, Dr. O. Lukin, Prof. Dr. A. D. Schlüter
Department of Materials, Institute of Polymers
HCI 541, ETH Zürich, 8093 Zürich (Switzerland)
Fax: (+41) 44-633-1395
E-mail: oleg.lukin@mat.ethz.ch
dieter.schluter@mat.ethz.ch

[b] Prof. Dr. A. Rossi
Department of Inorganic and Analytical Chemistry
University of Cagliari, 09100 Cagliari (Italy)

[c] R. Fiolka, Prof. Dr. A. Stemmer
Professur für Nanotechnik, ETH Zürich
8092 Zürich (Switzerland)

[d] Dr. K. Kita-Tokarczyk, Prof. Dr. W. Meier
Department of Chemistry, University of Basel
Klingelbergstr. 80, 4056 Basel (Switzerland)

Supporting information for this article is available on the WWW under http://dx.doi.org/10.1002/chem.200800478.

the desired lateral polymerizations. These monomers serve to prove the principle, but may not yet have the optimum molecular structures for the achievement of completely regular (periodic) 2D polymers and, perhaps even more importantly, the polymers' unequivocal structure proof.[1]

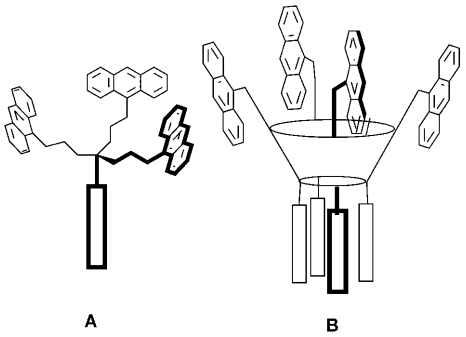

Figure 1. Schematic representation of monomer structures discussed in this work. Rectangles in both structures indicate hydrophilic groups that should help render the monomers spreadable at the air/water interface.

We describe the synthesis of some representatives of the compound families **A** and **B** and their spreading behavior at the air/water interface. Of those forming stable and reversibly compressible monolayers, one was selected for the next step, the photochemical treatment of its compressed monolayer. This treatment led to a covalent connection between the individual monomer units so as to render the layer a mechanically stable entity. The transfer of the untreated monolayer onto a solid substrate (oxidized silicon wafers) and the subsequent analysis of its composition and orientation on the substrate by the angle-resolved X-ray photoelectron spectroscopy (ARXPS) is discussed, as well as the determination of its thickness by ellipsometry and XPS. We also describe how the monolayer, photochemically treated at the interface, was analyzed in terms of thickness and mechanical stability by using ellipsometry (after transfer) and scratching experiments, respectively. The important aspect of stability was addressed by transferring the treated monolayer onto an electron microscopy grid with 2025 μm^2-sized holes to see whether they could be spanned by this film. Finally, we present model studies on photodimerizations of some relevant anthracene derivatives, mainly to help analytical aspects, which will be important for future work.

Results and Discussion

Monomer synthesis: The synthesis of potential group **A** monomers started from the commercially available 9-anthracene carboxylic acid **1**, which was reacted with the trisamino hydroxyl compound **2** to give alcohol **3** in 50% yield and on the 3-g scale (Scheme 1). Product **3**, referred to in the following as tripod, carries three anthracene units for dimerization reactions and a free hydroxyl function and was used to

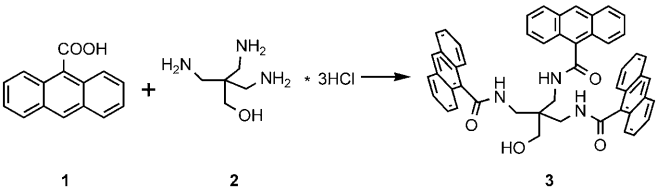

Scheme 1. Benzotriazol-1-yl-oxytripyrrolidinophosphonium hexafluorophosphate (PyBOP), *N*,*N*-diisopropylethylamine (DIPEA), CH_2Cl_2, DMF.

prepare a small collection of tripods with different polar groups so as to explore which specific structure shows the best spreading behavior at the air/water interface. Schemes 2–4 summarize the steps taken. The attachment of

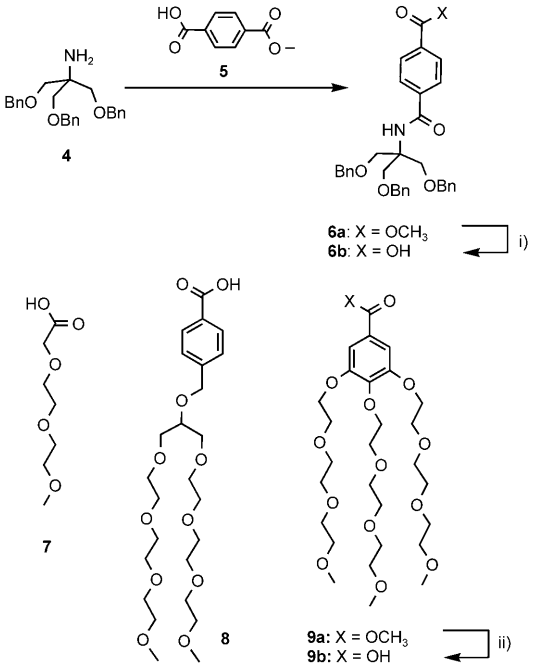

Scheme 2. i) KOH, MeOH/THF, H_2O; ii) KOH, MeOH/THF, H_2O.

the polar units **6b**, **7**, **8**, and **9b** proceeded best by using esterification with the 4-(dimethylamino)-pyridinium 4-toluenesulfonate (DPTS)/1-ethyl-3-(3-dimethylaminopropyl)-carbodiimide (EDC) system (see Supporting Information). This afforded the corresponding monomers **10**–**12** and **13b**, respectively, in yields of 30–50%. In addition to these tripods, calix[4]arene-based tetrapods were also synthesized. Calixarenes **16a** and **16b**, representing group **B** monomers, were prepared from starting materials **14a** and **14b** by reacting them with anthracene-9-carbaldehyde to furnish the Schiff bases **15a** and **15b**, whose reduction with $NaBH_4$ gave the desired compounds **16a** and **16b** on the 100-mg scale. The purification of the intermediates **15** turned out to be somewhat problematic in that they quickly hydrolyzed on column. This problem could be overcome, however, by

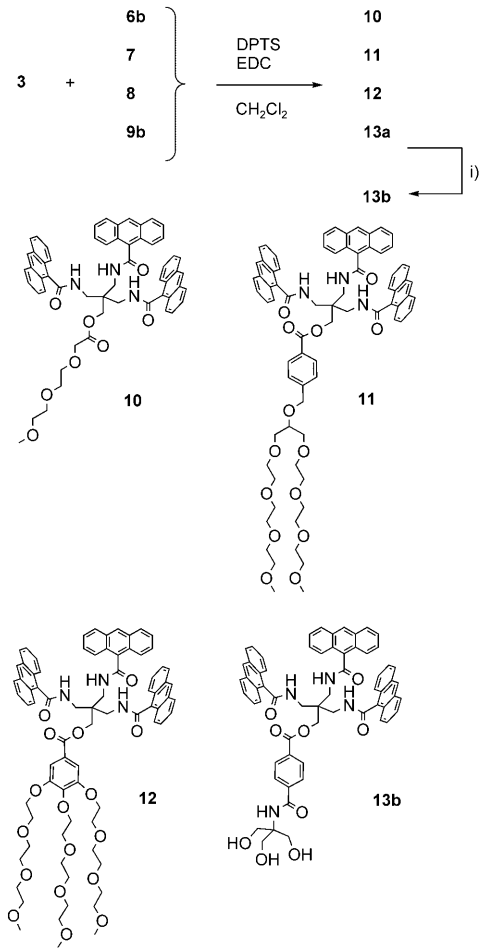

Scheme 3. i) Pd/C, H_2, EtOAc/MeOH.

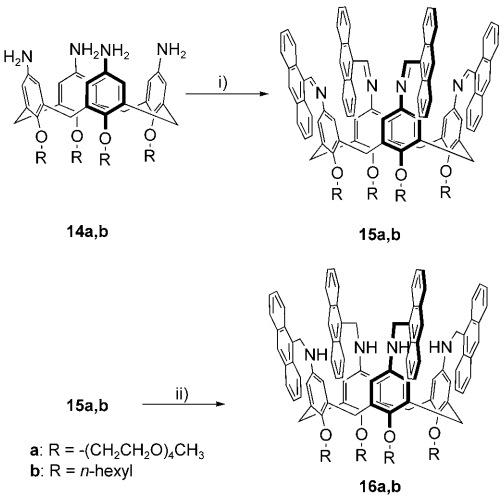

Scheme 4. i) Anthracene-9-carbaldehyde, dry MeOH; ii) $NaBH_4$, MeOH.

adding 5% triethylamine to the eluent. All new compounds were fully characterized.

Model photodimerizations: The photodimerization of anthracene and its derivatives has been studied in great detail,[9] including experimental conditions, regio- and stereochemical course, reversibility,[10] and accessible yields. Comprehensive reviews on this matter are available.[11] Besides simple derivatives, complex compounds containing anthracene units were also investigated. This involved the use of anthracenes as monomer units in polymer synthesis,[12] as cross-linking units in polymer network formation,[13] as well as in dendrimers[14] and other topologically unusual compounds.[15] By and large, dimerizations take place across the 9,10-positions and in the case of 9-substituted derivates, head/tail dimers are the preferred products, though exceptions for both behaviors have been described.[16] Yields of the photodimerization range typically from 40–70%. Though this may be considered insufficient for the ambitious goal described in the introduction, it should be pointed out that these figures refer to products formed under homogenous solution conditions. If photodimerization is applied to compressed monolayers in which the monomers are at tight, ideally almost van der Waals distance, higher yields for the coupling are to be expected. This is supported by reports that yields may go up for dimerizations of anthracenes in constrained geometries.[17] Scheme 5 shows the dimerizations that were studied in the frame of the present research.

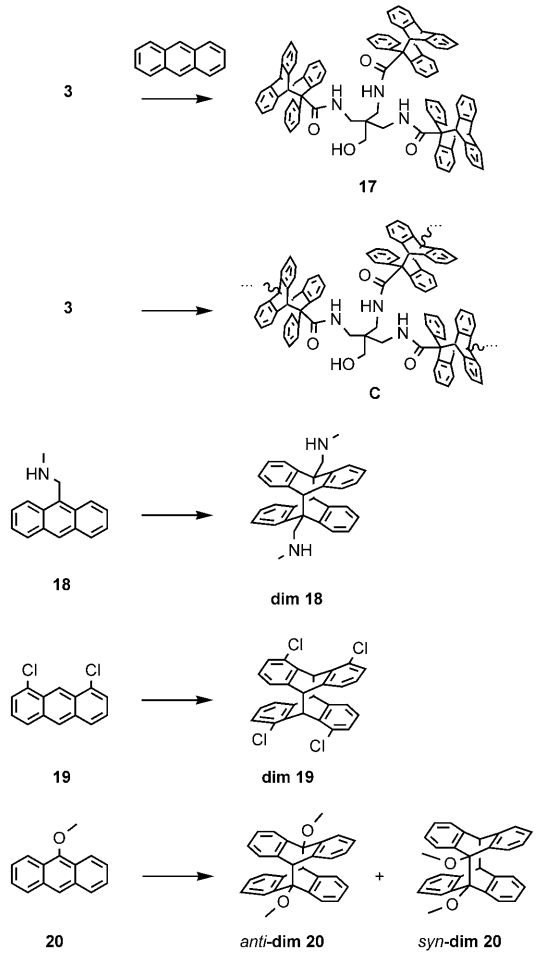

Scheme 5. Test and model studies performed with tripod **3** and the literature-known anthracenes **18**–**20**.

The question of how many of the functional groups (anthracenes) of the several oligofunctional compounds synthesized in the present study can actually be engaged in dimerizations was addressed using tripod **3**. This has the least complicated substitution pattern of all compounds and it was, therefore, expected that work-up and purification of the model reactions' products would be easier than for those representatives with flexible alkyl and oligoethyleneoxy (OEO) chains. At first, compound **3** was irradiated with a fivefold excess of parent anthracene per anthracene functionality in dichloromethane at 20 °C for 12 h. Product **17** was isolated by column chromatography and obtained reproducibly as colorless solid in yields of 45–50 %. Other products were formed, but these were neither isolated nor identified.[18]

The structure proof for **17** is based upon NMR spectroscopy and mass spectrometry results, but also the correct data from elemental analysis. Figure 2a and b compare its solution ^{13}C NMR spectrum with starting material **3**. Especially indicative are the new signals at approximately $\delta =$ 142, 66, and 55 ppm which correspond to the *ortho*-phenylene units and the bridgehead carbons, respectively. Thus, all three anthracene moieties of **3** were individually engaged in dimerization reactions and it was thus assumed that the other tri- and tetrapods would behave similarly.

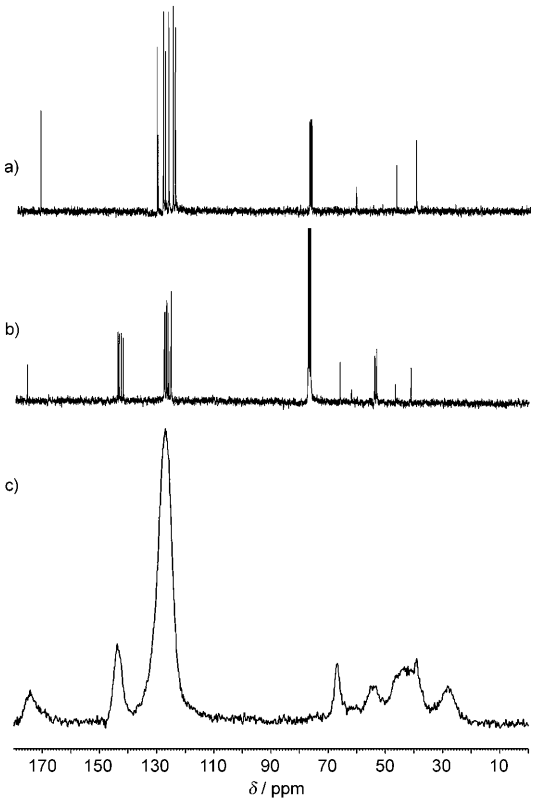

Figure 2. Solution ^{13}C NMR spectra of starting tripod **3** (a) and its threefold anthracene adduct **17** (b), and solid-state cross polarization magic angle spinning (CPMAS) ^{13}C NMR spectrum of network **C** formed by the tripod's self-addition reaction (c).

In a future stage of the project it will be important to prove that anthracene dimerization takes place at the air/water interface when spread and compressed monolayers are irradiated. Because under such conditions just a very small quantity of molecules is involved, the analytical tools applied need to account for this. Grazing incidence IR spectroscopy (GI-IR) is a powerful tool for monolayer characterization and it was thus a prime task to obtain IR spectra of relevant compounds as a reference for these future studies. The top part of Figure 3 compares sections of the IR spectra

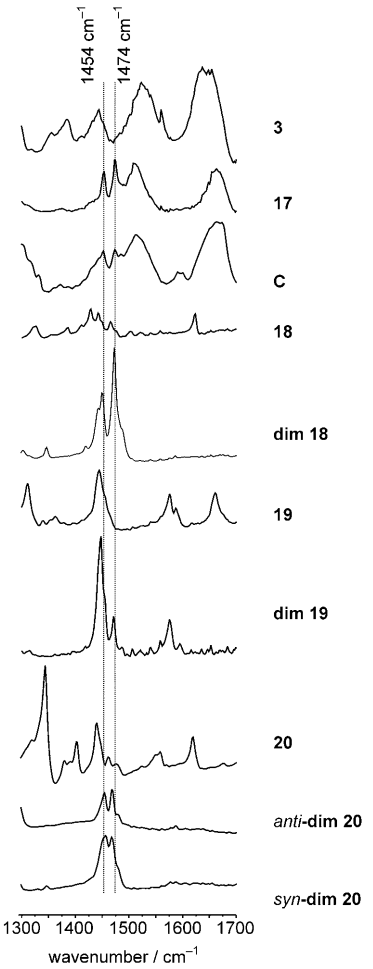

Figure 3. IR spectra in KBr of the four anthracenes **3**, **18**, **19**, and **20** and their dimerization product(s) **17** and **C**, **dim-18**, **dim-19**, as well as *ht* **dim-20** and *hh* **dim-20**, respectively. Despite the rather different substitution patterns, all dimers show two signals at or near 1454 and 1474 cm^{-1}.

(in KBr) of starting compound **3** with **17**. Evidently, the dimerization is associated with the appearance of absorptions at 1454 and 1474 cm^{-1}, as was already reported for hydrocarbon cages closely related to the one contained in **17**.[11,19] Because of the anticipated importance of this analytical aspect, three other anthracene derivatives, **18**–**20**, were also synthesized (see Experimental Section) and photochemically dimerized into their *head*/*tail* (*ht*) dimers [**dim-18** (for an X-ray structure, see Supporting Information), **dim-19**] and iso-

meric *head/head* (*hh*) and *ht* dimers for **dim-20**.[20] This latter mixture was separated into the individual components. The respective IR spectra are also compiled in Figure 3. As can be seen, all dimers exhibit these two signals at almost the same wave numbers to the ones above. This applies also to the two different *hh* and *ht* stereoisomers of **dim-20**, which is somewhat unfortunate. It was hoped that GI-IR spectroscopy would enable extraction of information not only about whether or not dimerization has taken place in a monolayer at the air/water interface, but also about the stereochemistry of the product.[21,22] The UV spectrum of **17** confirmed the complete disappearance of all anthracene-typical absorptions (Figure 4a).

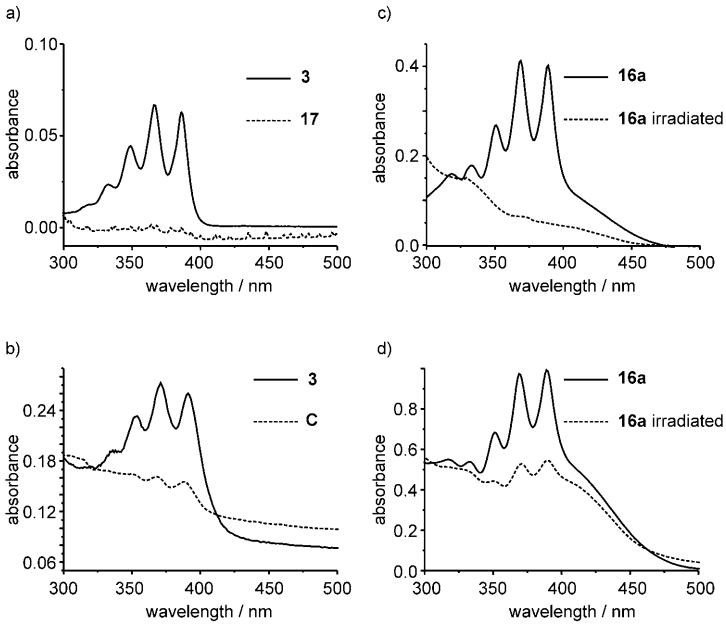

Figure 4. UV spectra in chloroform comparing tripods **3** and **17** (a), tripod **3** and network **C** (b), tetrapod **16a** and the product of its irradiation in highly diluted (0.1 mM) (c), and highly concentrated (125 mM) CH_2Cl_2 solutions (d).

Next, the reaction of **3** with itself was studied. This was necessary because this self-addition involves only monosubstituted anthracenes (at C-9) rather than a monosubstituted one and the parent anthracene. This could result in a reduced propensity to undergo self-dimerization. It was expected that if dimerization worked, an insoluble network should form, the formula **C** of which (Scheme 5) for simplicity considers neither eventual *hh* dimers nor incomplete reactions. A 10-mM dichloromethane solution of **3** was irradiated at 20 °C for 12 h under nitrogen during which time a precipitate formed. This was filtered off (approx. 77 % of total mass) and the supernatant solution was concentrated up to give a complex mixture of compounds (approx. 23 % of total mass). The precipitate's solid-state ^{13}C NMR spectrum (Figure 2c) shows signals at approximately $\delta = 144$ ppm as well as $\delta = 67$ and 55 ppm that correspond to the *ortho*-phenylene units and the bridgeheads, respectively, very much like model compound **17**. Network **C** also shows anthracene signals in the UV range (measured in reflection) indicative of unreacted (end) groups (Figure 4b). The intensity of these signals was not quantified. In addition, the IR spectrum exhibits the characteristic signals at 1454 and 1474 cm^{-1}. Thus, the expected network had formed at least for the major part of the material.

The reactivity of compound **16a** under irradiation was also briefly investigated using UV spectroscopy. The outcome of these reactions depended strongly on concentration. For highly diluted dichloromethane solutions (0.1 mM) a soluble product was obtained that gave the UV spectrum depicted in Figure 4c. The anthracene-typical resonances had disappeared, suggesting that under these highly diluted conditions a twofold intramolecular dimerization took place. Such reactions have been reported for simpler systems with just two anthracene units.[23] At much higher concentrations (125 mM) a precipitate formed, whose UV spectrum (Figure 4d) was taken in reflection. As for the self-addition of compound **3**, some residual anthracene signals were detected and tentatively ascribed to end groups.

Experiments and analyses at air/water and air/solid interfaces

Non-polymerized monolayers: The ability of a compound to form stable Langmuir monolayers depends on its solubility and the amphiphilic (hydrophilic-to-hydrophobic) balance. Film formation was tried with compounds **3**, **10**–**12**, **13b**, and **16a** using conventional techniques (see Experimental Section). Compound **3** (hydrophobic) formed films, however, these were not reversible and rather crystalline; compounds **10**–**12** (hydrophilic) did not spread but rather submerged into the subphase. Compounds **13b** and **16a** formed stable, compressible films with different reversibilities, with that of **16a** being superior. The surface-pressure/-area isotherms of both compounds are depicted in Figure 5. The full isotherm

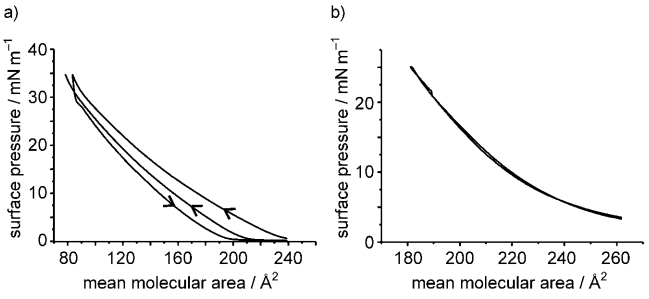

Figure 5. Surface-pressure/-area isotherms for monomers **13b** (a) and **16a** (b) at the air/water interface. Arrows indicate compression and expansion isotherms.

of **16a** can be found in the Supporting Information (Figure S2). On the basis of these curves, monomer **16a** was selected for the initial polymerization experiments. First the area per molecule was estimated. For this purpose a tangent

was drawn near the surface pressure of 25 mN m^{-1}, which intersected the x-axis at approximately 2.2 nm^2. An alternative value was obtained by measuring the area at this pressure, which was found to be 1.85 nm^2. From the two extreme conformations of stick models shown in Figure 6, the expected

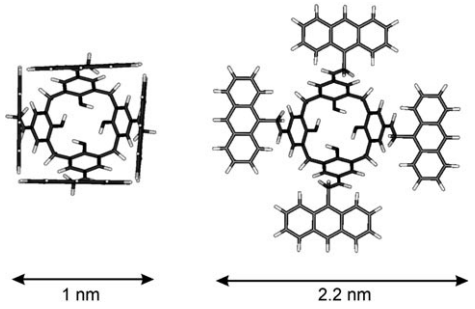

Figure 6. Molecular models of the two extreme conformations of monomer **16a** with the four anthracene units in upright (left) and horizontal (right) orientations, respectively. The areas covered by these two conformers differ significantly between approximately 1.0 and 4.8 nm^2.

value should be somewhere between 1.0 and 4.8 nm^2. An intermediate value is suggested by the X-ray structure of compound **16b** (Figure 7). This compound was chosen because it

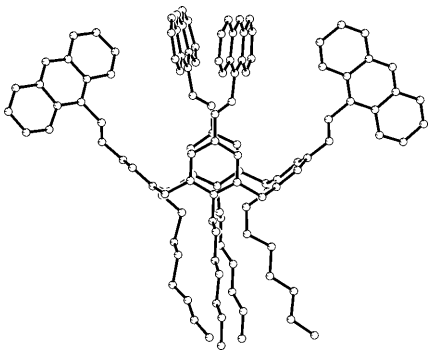

Figure 7. X-ray molecular structure of calix[4]arene **16b**, which serves as a model for **16a**, showing that in the crystal this compound attains an area between the two extreme models for **16a** shown in Figure 6.

was easier to grow single crystals from it than from **16a** and the anthracene geometry should not be affected much by the substitution at the lower rim. It is apparent that the relative orientation of the anthracene moieties in **16a** at the interface needs to be different from that of the same units in the single crystal of **16b**, if a high degree of intermolecular [4+4] dimerizations is to be brought about.

The film formation upon increasing surface pressure was monitored by Brewster angle microscopy (BAM). As can be seen from the representative snapshots depicted in Figure 8, for low pressures homogenous areas are initially separated by less-ordered stripes. However, at higher pressure (typically 25 mN m^{-1}), a fully homogenous film of **16a** was observed, which was used for all transfers and also irradiations.

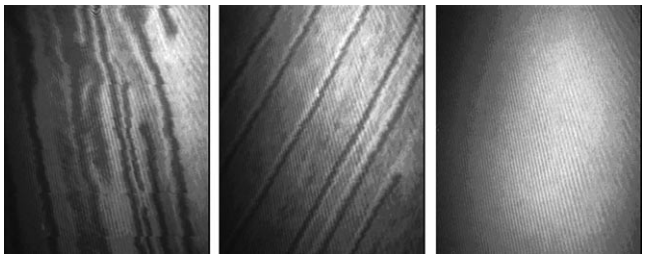

Figure 8. Brewster angle microscopy images of film formation during increase in surface pressure. The rightmost image indicates a rather smooth monolayer that represents the state at which transfers and irradiations were performed. The size of the images is 430 μm × 498 μm.

Although the isotherm indicated that at 25 mN m^{-1} the film of **16a** should still be a monolayer, this was confirmed by ellipsometry measurements of Langmuir–Blodgett layers transferred on oxidized silicon wafers; each time, a single layer was transferred upon the dipper upstroke. These measurements were carried out at three points and representative results are compiled in Table 1 (entries 1–3). The average

Table 1. Thickness [Å] of transferred monolayers of **16a**.

Entry	Vertical transfer		Horizontal transfer	
	Monolayer	UV-treated monolayer	Monolayer	UV-treated monolayer
1	18	20	17	21
2	19	20	18	20
3	19	20	17	21
4	19±1	20±1	17±1	21±1

height of the film was found to be in the order of (19±1) Å (Table 1, entry 4, left column). This value corresponds well with the height of the individual molecule **16a**, assuming that its flexible chains are somewhat contracted and not in the all-*trans* conformation.[24] This assumption is reasonable considering the fact that both the oligoethyleneoxy (OEO) chains and the substrate are polar. The film height was also checked by Langmuir–Schäfer transfer, which gave a slightly smaller value of (17±1) Å (Table 1, entry 4, third column).

Next, XPS measurements were performed aiming at compositional, structural, and orientation information of this monolayer. Figure 9 shows the survey spectrum collected of a monolayer of **16a** transferred onto a silicon substrate. Carbon, oxygen, and nitrogen signals are detected together with the Si2s and Si2p that are due to the substrate. The nitrogen signal, N1s, indicates a successful transfer of the monolayer as this element is the only one that is exclusively present in the monomer. Because no other signals are detected, it can also be concluded that the monolayer is free of contamination. Detailed spectra of C1s, O1s, N1s, and Si2p were also taken (Figure S3) and the peak areas used to calculate atomic concentrations and monolayer thickness. The Si2p spectrum exhibits two signals, one at 99.4 eV and another one at 103.4 eV. The first signal is due to the parent

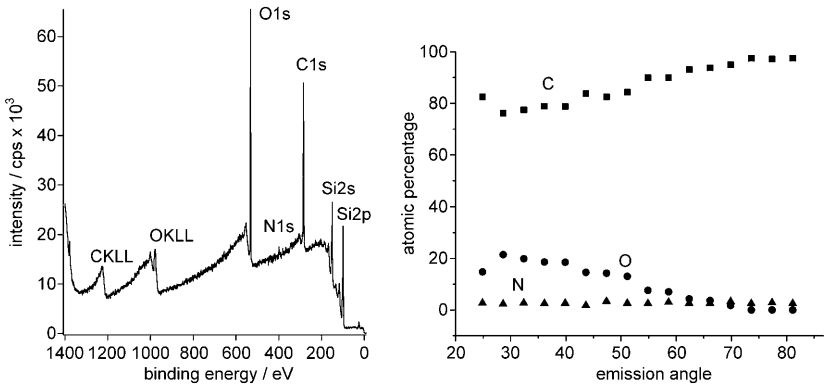

Figure 9. Survey XPS spectrum of a non-polymerized monolayer of **16a** transferred onto an oxidized silicon wafer (left), and apparent atomic concentration vs. emission angle of non-polymerized monolayer of **16a** transferred onto an oxidized silicon wafer (right). The apparent concentration is the concentration assuming a homogenous compound within the analyzed depth. If the concentration of an element increases as emission angle increases (e.g., carbon) then it is mainly present at the outer part of the analyzed volume (data acquired with the Theta Probe Thermo, Fisher).

substrate and the second can be assigned to silicon dioxide.[25]

The O1s spectrum contains the contributions of both the silicon dioxide at 533.1 eV and the monolayer of monomer **16a**. In fact, the signal that is symmetric in the case of pure silicon dioxide shows here a non-symmetry at the lower-binding-energy side due the presence of oxygen signals of the monolayer. The components at 532.6 and 533.3 eV were identified by least-square peak-synthesis routine using the fitting parameters obtained on the basis of reference samples: the untreated monolayer and the drop-cast compound analyzed using the same spectrometer settings. These were assigned to the C-O-C chains and to the Ar–O, respectively. These values are in agreement with the literature.[26] The C1s signal is also non-symmetric as it contains the signals due to the aromatic rings (284.7 eV) of the calixarene, the anthracenes (285.5 eV), and the C-O-C units at 286.7 eV[26] The binding-energy value of the anthracene units of the monolayer is lower than that of parent anthracene (not shown here); this shift is attributed to the presence of the donor substituents in the former.

The N1s signal is symmetric at 400.4 eV. This value is 3.4 eV higher than that measured on the pure drop-cast compound, suggesting that the nitrogen atom might be bonded to water molecules. The atomic composition of the monolayer was based on the line intensities determined by integration of the fitted Gaussian/Lorentzian model functions after a Shirley background subtraction and corrected for the photoionization cross-sections, the asymmetry function, the mean free path, and the transmission function of the spectrometer. The values (%) found: C 82.5, N 2.7, O 14.8, are in good agreement with the calculated values (%): C 83.8, N 2.7, O 13.5. The monolayer thickness was calculated to be (26 ± 0.1) Å, which is significantly larger than the values obtained by ellipsometry, even if it is still in agreement with the assumption of a monolayer. The difference might be due to the fact that the density does not feature in this calculation: a more appropriate model, such as the three-layer model, would require knowledge of the monolayer density.[27]

Finally, angle-resolved XPS measurements were carried out on **16a** to get an insight into the monolayer's orientation. Figure 9 shows the plot of the atomic concentration vs. the emission angle, whereby the latter is the one formed by the direction of the emitted electrons with the surface normal. This plot suggests that the C-O-C units of the monomers are in the inner part of the film whereas the carbon species seem to be located in the outer part of the monolayer. Thus, the monolayer has an orientation as one would have intuitively suggested.

Polymerized monolayer: With this information at hand, the first irradiation experiments were performed. A monolayer of **16a** was compressed to 27 $mN\,m^{-1}$ and irradiated for 30 minutes with unfiltered UV light of a medium-pressure mercury lamp that was positioned above the film at a distance of approximately 20 cm. This distance was kept constant throughout all irradiations described in this paper. The whole trough was placed inside a box, which allowed application of gentle nitrogen flow during the entire irradiation time to exclude peroxide formation. First, it was tested whether irradiation has any effect on the appearance of the BAM images. Figure 10 compares images before and after irradiation. As can be seen, there was no difference at all, even though the image of the treated film was taken after the barriers had been opened. To test whether cross-linking had actually taken place, both the treated and non-treated monolayers were scratched with a needle and the responses compared.

Both responses were monitored by BAM. Whereas without irradiation the "wounds" healed instantaneously (not shown), those in the treated film remained completely unchanged, even if the barrier was opened. This proves the non-treated film to behave like a fluid and the treated one to be covalently cross-linked. It should be stressed that these experiments do not enable conclusions to be drawn regarding how many of the anthracenes were actually involved and whether a periodic structure was formed. These important questions are presently being pursued.[19] Next, the irradiated film was transferred onto silica and the height measurement repeated. As can be seen from Table 1, the values are (20 ± 1) Å for the vertical and (21 ± 1) Å for the horizontal transfers. Clearly, the irradiation process did not change the monolayer nature of the film, though there may be some thickening.

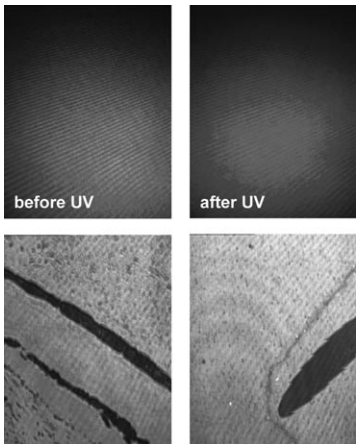

Figure 10. BAM images of non-irradiated (top left) and UV-irradiated monolayer of **16a** at the air/water interface (top right) indicating that irradiation does not cause morphological changes and crack formation visible by BAM. BAM images of UV-irradiated monolayers of **16a** after scratching with a needle (bottom left and right). The "wounds" stay unchanged even if the film is decompressed. The size of the images is 430 μm × 498 μm.

The transferred and cross-linked monolayers were also investigated by contact-angle measurements with water. From the XPS measurements it was expected that this layer should show the anthracene units at the top to be at least partially dimerized. Contact angles for self-assembled monolayers (SAMs) with aromatic units at their surface are known to be in the order of 80–85°.[28] Measurements on our films directly after transfer reproducibly gave contact angles between 32–45°. These values showed considerable scatter and were clearly too low. However, after drying the samples under high vacuum, the values were reproducibly between 82–88° and, thus, well within the expected range. This substantial change of contact angle upon drying is explained by adsorbed water, which in the non-dried samples is abundantly available (OEO chains!) and can reach the surface through the many pores necessarily present in the cross-linked film.

To test the mechanical stability of the cross-linked monolayer, transfers on electron microscopy grids with holes sized 45 × 45 μm were performed to see whether they can be covered with films without rupture. The literature describing ultrathin layers over-spanning holes is scarce.[29] Attempts with Langmuir–Blodgett transfer were unsuccessful, however, the horizontal transfer (Langmuir–Schäfer method) was successful. However, it should be noted that not every transfer was actually successful; only approximately every fifth transfer gave usable results. Figure 11 compares an unsatisfactory and a rather successful transfer. The images were taken with a conventional optical microscope and the contrast is based on interference. In the first case, practically all films over holes are ruptured. Note that the direction of the cracks is more or less the same, which seems to indicate that during coverage a stress was applied to the entire film while near the grid. To say this crack formation is associated with drying effects is merely speculation. In a blind test, also the

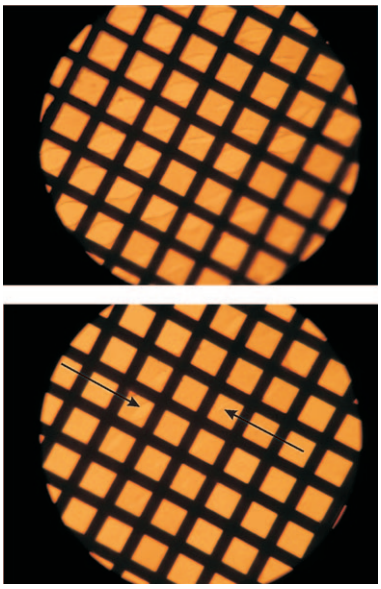

Figure 11. Light-microscopy images of transferred UV-treated monolayers of monomer **16a** on a Cu grid with holes sized 45 × 45 = 2025 μm^2. The top image shows a case considered unsuccessful because film rupture could not be prevented, the bottom image represents a successful case because many holes are over spanned by non-ruptured films. The arrows point towards cracks.

non-cross-linked film was transferred onto such a grid, however, in none of many attempts was it possible to cover holes, not even for small parts. Cross-linking is thus a prerequisite for such experiments with films from **16a**. The transferred films are stable for at least several days under ambient conditions. The differential interference contrast (DIC) micrograph (Figure 12) shows a film five days after transfer, with no visible change detected. Some of the grid holes are covered (right-hand side) and some are not (left-hand side). The holes in the center are (still) partially covered; due to rupture, the film in part folds back on itself, wrinkles, and shows a tendency to roll up at the edge.

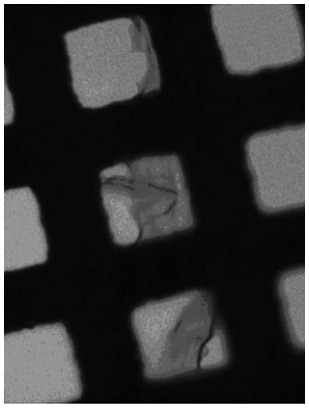

Figure 12. DIC image (×40) of a cross-linked monolayer of **16a** taken 5 days after the transfer event. The film is on a Cu grid with 2025 μm^2-sized holes, some of which are spanned over by non-ruptured films (holes on the right-hand side) and others are not at all (holes on the left-hand side). The holes in the center are partially covered by films and overlaying parts, wrinkles, and rolled-up edges are visible.

Conclusion

Monomer **16a**, decorated with four anthracene units, spreads reversibly at the air/water interface, and after compression to 25 $mN\,m^{-1}$ can be photochemically cross-linked into a sheet-like object, whose mechanical stability is sufficient to allow transfer onto both a solid substrate and a Cu grid with 2025 μm^2 sized holes. These holes can actually be spanned over, whereby the films remain unchanged under ambient conditions at least for several days. The sheets have the thickness of a monolayer and two different faces, one that consists of more or less dimerized anthracene units and the other of oligoethyleneoxy chains. Thus, the sheets are amphiphilic. Based on these results the next steps involve 1) proving the level of order in the sheet by grazing incidence X-ray diffraction and IR spectroscopy, the near field microscopies, as well as other techniques, 2) design and testing of other monomers that may have an even higher chance to lead to sheets with long-range positional order and periodic bonding patterns,[1] 3) testing properties such as rupture forces.

Experimental Section

General: The elemental analyses were performed using a Leco CHN-900 or Leco CHNS-932 instrument. The melting points were measured in open capillaries by using a Büchi B-540 and were uncorrected. MALDI-TOF mass spectra were recorded by using an electron-ionization (EI) MS spectrometer (Micromass AutoSpec-Ultima) or a FTMALDI MS spectrometer (IonSpec Ultra Instrument). ^1H- and ^{13}C NMR spectra were recorded by using Bruker Avance 300 and 500 MHz spectrometers at RT in the indicated deuterated solvents, which were purchased from Merck or Deutero GmbH. The resonance multiplicities in the ^1H NMR spectra are described as s (singlet), d (doublet), t (triplet), and m (multiplet). Broad resonances are indicated by br. Reactions were monitored by TLC using TLC silica-coated aluminium sheets Alugram by Macherey–Nagel (SIL-G/UV_{254}). The compounds were visualized by applying 254 or 366 nm UV light. Column chromatography purifications were performed with silica gel, BIO-RAD Bio-Beads S-X1 [200–400 mesh], or preparative recycling GPC (Japan Analytical Industry Co. Ltd., LC 9101) equipped with a pump (Hitachi L-7110, flow rate 3.5 $mL\,min^{-1}$), a degasser (GASTORR-702), a RI detector (Jai RI-7), a UV detector (Jai UV-3702, $l = 254$ nm), and two columns (Jaigel 2H and 2.5H, 20×600 mm for each) using chloroform as eluent at RT. Optical microscopy experiments were carried out by using a Leica DM-RP. FTIR measurements were performed by using a Bruker Vector 22 instrument in KBr pellets. UV/Vis spectra were recorded by using a Perkin–Elmer UV/Vis Lambda 20 spectrometer.

Langmuir monolayers: Monolayers of **16a** were prepared by spreading an aliquot of a solution (1 $mg\,mL^{-1}$ in $CHCl_3$; spectroscopy-grade solvents) on Millipore water of pH 6 on a mini Langmuir–Blodgett trough (total area 242 cm^2, from KSV, Finland), placed on an anti-vibration table in a dust-reduced environment (no clean-room). After spreading, the solvent was allowed to evaporate for 5 min, followed by compression of the film at 10 $mm\,min^{-1}$. The surface pressure of the monolayers was measured at a precision of ± 0.01 $mN\,m^{-1}$ with a Wilhelmy plate (chromatography paper, ashless Whatman Chr 1) on an electrobalance. Monolayers were compressed at 22 °C.

Irradiation and transfer of monolayers: An UV 250-Watt lamp fitted with a Gallium bulb from UV Light Technology was placed over the trough at a distance of 20 cm. The time of irradiation was 30 min. During irradiation the whole set-up was purged with a gentle stream of nitrogen. Langmuir–Blodgett and Langmuir–Schäfer transfer were performed according to the protocol.[30] For the Schäfer transfer a Cu grid purchased from Plano with a pitch of 45 mm was used.

Brewster angle microscopy: Monolayer morphology was visualized by using a BAM2plus Brewster angle microscope (Nanofilm, Germany), with a 50-mW laser at the wavelength of 532 nm. With a 10× Nikon long-distance objective, the microscope has a resolution of 2 μm; recorded images correspond to 430 μm in width.

Ellipsometry: The dry thicknesses of the films were determined by variable angle spectroscopic ellipsometry (VASE, M-2000F, L.O.T. Oriel GmbH, Germany). Measurements were conducted under ambient conditions at three angles of incidence (65, 70, and 75°) in the spectral range of 370–995 nm. Measurements were fitted with the WVASE32 analysis software using a three-layer model for an organic layer on a silicon substrate.

X-ray photoelectron spectroscopy: Small-area X-ray photoelectron spectra (XPS) and angle-resolved XPS (ARXPS) were acquired using a Theta Probe (Thermo Fisher Scientific, Waltham MA, USA). The residual pressure during the analysis was 10^{-7} Pa. The measurements were carried out using an $Al_{K\alpha}$ (1486.6 eV) radiation source run at 70 W, 400-μm beam diameter. The emitted electrons were collected by using a radian lens with a conical angle of acceptance of ca. 3°. The emission angle ranges from 23 to 83°. The spectra of O1s, C1s, N1s, Si2s, and Si2p were obtained in constant analyzer transmission mode with a pass energy of 50 eV and a step size of 0.1 eV (full width at half maximum height, FWHM, for $Ag3d_{5/2} = 0.7$ eV). The angular information was summed into 16 channels.

The survey spectra were acquired with a pass energy of 100 eV. The instrument was calibrated using the inert-gas-ion-sputter cleaned reference materials SCAA90 of Cu, Ag, and Au.10 following ISO 15472. Sample charging was corrected by referring all binding energies to the carbon 1s signal at 285.0 eV.

Contact-angle measurements were carried out by using a Ramè-hart, Inc. NRL C.A. Goniometer (Model No 100–00–230). All reported values are the average contact angles at three different spots per sample determined by sessile drop technique.

Synthesis

Compounds **1**, **5**, **7**, **18**, and the parent anthracene were purchased from commercial sources and used without additional purification. Compounds **2**,[31] **4**,[32] **9a**,[33] **14a**,[34] **14b**,[35] **19**,[36] **20**,[37] and **dim-20**[20] were prepared according to the literature procedures. Preparation and characterization of the remaining compounds is given in the Supporting Information.

General procedure for esterification: Alcohol (1.45 equiv) and DPTS (1.45 equiv) were added to a solution of acid (1 equiv) in a mixture of dry CH_2Cl_2 and dry DMF at RT. After 15 min EDC (1.45 equiv) was added and the mixture was stirred at RT overnight. The reaction mixture was diluted with CH_2Cl_2 and washed twice with brine. The organic layer was separated and dried over $MgSO_4$. The solvent was removed under reduced pressure. The crude product was purified by silica gel column chromatography or GPC.

General procedure for the dimerization of anthracene derivatives: The compound was dissolved in dichloromethane and then the solution was degassed. The degassed solution was irradiated with UV light for 12 h. Then the solvent was removed under reduced pressure and subjected to the preparative GPC purification.

CCDC 680390 and 680391 contain the supplementary crystallographic data for this paper. These data can be obtained free of charge from The Cambridge Crystallographic Data Centre via www.ccdc.cam.ac.uk/data_request/cif.

Acknowledgements

This research was supported by the Schweizer Nationalfonds (200021-111739 and 200020-117572) and ETH grants (TH-05 07-1). We wish to

thank cordially several people for their support of this research: Prof. G. Wegner, MPI-P, Mainz; Prof. H. Möhwald, MPI-KG, Golm; Prof. V. Böhmer, Mainz University; Dr. G. Brezesinski, MPI-KG, Golm; Dr. K. Wagner, MPI-KG, Golm; Dr. W. B. Schweizer, B. Malisova, ETHZ; C. Zink, ETHZ.

[1] J. Sakamoto, J. van Heijst, O. Lukin, A. D. Schlüter, *Angew. Chem.* in press, DOI: 10.1002/ange. 200801863; *Angew. Chem. Int. Ed.* in press, DOI: 10.1002/anie.200801863.

[2] For finite, periodic 2D compounds, see: a) H.-J. Räder, K. Müllen, *Anal. Chem.* **2000**, *72*, 4591–4597; b) D. Wasserfallen, M. Kastler, W. Pisula, W. A. Hofer, Y. Fogel, Z. Wang, K. Müllen, *J. Am. Chem. Soc.* **2006**, *128*, 1334–1339; c) J. Anthony, A. M. Boldi, Y. Rubin, M. Hobi, V. Gramlich, C. B. Knobler, P. Seiler, F. Diederich, *Helv. Chim. Acta* **1995**, *78*, 13–45; d) F. Diederich, *Nature* **1994**, *369*, 199–207; e) J. A. Marsden, M. M. Haley, *J. Org. Chem.* **2005**, *70*, 10213–10226.

[3] For double- and oligostranded polymers, see: a) L. Blanco, H. E. Nelson, M. Hirthammer, H. Mestdagh, S. Spyroudis, K. P. C. Vollhardt, *Angew. Chem.* **1987**, *99*, 1276–1277; *Angew. Chem. Int. Ed. Engl.* **1987**, *26*, 1246–1247; b) V. R. Sastri, R. Schulman, D. C. Roberts, *Macromolecules* **1982**, *15*, 939–947; c) A. D. Schlüter, M. Löffler, V. Enkelmann, *Nature* **1994**, *368*, 831–834; d) B. Schlicke, H. Schirmer, A. D. Schlüter, *Adv. Mater.* **1995**, *7*, 544–546; e) A. Godt, A. D. Schlüter, *Adv. Mater.* **1991**, *3*, 497–499; f) U. Scherf, K. Müllen, *Makromol. Chem. Rapid Commun.* **1991**, *12*, 489–497; g) M. B. Goldfinger, T. M. Swager, *J. Am. Chem. Soc.* **1994**, *116*, 7895–7896; h) J. M. Tour, J. J. S. Lamba, *J. Am. Chem. Soc.* **1993**, *115*, 4935–4936; i) J. Wu, L. Gherghei, M. D. Watson, J. Li, Z. Wang, C. D. Simpson, U. Kolb, K. Müllen, *Macromolecules* **2003**, *36*, 7082–7089; j) A. Tsuda, H. Furuta, A. Osuka, *Angew. Chem.* **2000**, *112*, 2649–2652; *Angew. Chem. Int. Ed.* **2000**, *39*, 2549–2552; k) A. Tsuda, A. Osuka, *Science* **2001**, *293*, 79–82.

[4] For non-covalent, coordinative 2D model structures, see: a) T. N. Milic, N. Chi, D. G. Yablon, G. W. Flynn, J. D. Batteas, C. M. Drain, *Angew. Chem.* **1998**, *114*, 2221–2223; *Angew. Chem. Int. Ed.* **1998**, *41*, 2117–2119; b) T. N. Milic, N. Chi, D. G. Yablon, G. W. Flynn, J. D. Batteas, C. M. Drain, *Angew. Chem.* **2002**, *114*, 2221–2223; *Angew. Chem. Int. Ed.* **2002**, *41*, 2117–2119; c) P. N. W. Baxter, J.-M. Lehn, J. Fischer, M.-T. Youinou *Angew. Chem.* **1994**, *106, 2432–2434; Angew. Chem. Int. Ed. Engl.* **1994**, 33, 2284–2287; *Angew. Chem. Int. Ed. Engl.* **1994**, *33*, 2284–2287; d) M. Barboiu, G. Vaughan, R. Graff, J.-M. Lehn, *J. Am. Chem. Soc.* **2003**, *125*, 10257–10265.

[5] For polymer-chemical approaches to 2D polymers using random-walk processes, see: a) S. Asakuma, H. Okada, T. Kunitake, *J. Am. Chem. Soc.* **1991**, *113*, 1749–1755; b) S. I. Stupp, S. Son, H. C. Lin, L. S. Li, *Science* **1993**, *259*, 59–62; c) S. I. Stupp, S. Son, L. S. Li, H. C. Lin, M. Keser, *J. Am. Chem. Soc.* **1995**, *117*, 5212–5227.

[6] For various approaches at interfaces, see: a) T. Takami, H. Ozaki, M. Kasuga, T. Tsuchiya, Y. Mazaki, D. Fukushi, A. Ogawa, M. Uda, M. Aono, *Angew. Chem.* **1997**, *109*, 2909–2912; *Angew. Chem. Int. Ed. Engl.* **1997**, *36*, 2755–2757; b) G. Sui, M. Micic, Q. Huo, R. M. Leblanc, *Colloids Surf. A* **2000**, *171*, 185–197; c) D.-J. Qian, C. Nakamura, J. Miyake, *Langmuir* **2000**, *16*, 9615–9619; d) D.-J. Qian, C. Nakamura, J. Miyake, *Chem. Commun.* **2001**, 2312–2313; e) Y. Okawa, M. Aono, *Nature* **2001**, *409*, 683–684; f) T. L. Markrova, B. Sundqvist, R. Höhne, P. Esquinazi, Y. Kopelevich, P. Scharff, V. A. Davydov, L. S. Kashevarova, A. V. Rakhmanina, *Nature* **2001**, *413*, 716–718; g) A. Miura, S. De Feyter, M. M. S. Abdel-Mottaleb, A. Gesquière, P. C. M. Grim, G. Moessner, M. Sieffert, M. Klapper, K. Müllen, F. C. De Schryver, *Langmuir* **2003**, *19*, 6474–6482; h) H.-G. Liu, X.-S. Feng, L.-J. Zhang, J. Jiang, Y.-I. Lee, K.-W. Jang, D.-J. Qian, K.-Z. Yang, *Mater. Lett.* **2003**, *57*, 2156–2161; i) S. Margadonna, D. Pontiroli, M. Belli, T. Shiroka, M. Ricco, M. Brunelli, *J. Am. Chem. Soc.* **2004**, *126*, 15032–15033; j) Y. He, Y. Chen, H. Liu, A. E. Ribbe, C. Mao, *J. Am. Chem. Soc.* **2005**, *127*, 12202–12203; k) J. Malo, J. C. Mitchell, C. Venien-Bryan, J. R. Harris, H. Wille, D. J. Sherratt, A. J. Turberfield, *Angew. Chem.* **2005**, *117*, 3117–3121; *Angew. Chem. Int. Ed.* **2005**, *44*, 3057–3061; l) D.-J. Qian, H.-T. Chen, B. Liu, X.-M. Xiang, T. Wakayama, C. Nakamura, J. Miyake, *Colloids Surf. A* **2006**, *284+285*, 180–186.

[7] For a recent review on graphenes, see: A. K. Geim, K. S. Novoselov, *Nat. Mater.* **2007**, *6*, 183–191.

[8] Natural graphene in its undisturbed domains meets our definition of a 2D polymer. See ref. [7].

[9] a) J. Bertran, G. H. Schmid, *Tetrahedron* **1971**, *27*, 5191–5200; b) D. O. Cowan, R. L. Drisko, *Elements of Photochemistry*, Plenum Press, New York, **1976**, Chapter 2; c) H. Sasaki, S. Kobayashi, K. Iwasaki, S. Ohara, T. Osa, *Bull. Chem. Soc. Jpn.* **1992**, *65*, 3103–3107; d) H. D. Becker, *Chem. Rev.* **1993**, *93*, 145; e) S. Grimme, S. D. Peyerimhoff, H. Bouas-Laurent, J. P. Desvergne, H. D. Becker, S. M. Sarge, *Phys. Chem. Chem. Phys.* **1999**, *1*, 2457–2462; f) S. Grimme, C. Diedrich, M. Korth, *Angew. Chem.* **2006**, *118*, 641–645; *Angew. Chem. Int. Ed.* **2006**, *45*, 625–629.

[10] The reversibility aspect is of special importance to the present project because it in principle allows unzipping of an entire molecular sheet into its components.

[11] a) H. Bouas-Laurent, A. Castellan, J. P. Desvergne, *Pure Appl. Chem.* **1980**, *52*, 2633–2648; b) J. P. Desvergne, N. Bitit, A. Castellan, M. Webb, H. Bouas-Laurent, *J. Chem. Soc. Perkin Trans. 2* **1988**, 1885–1894; c) J. P. Desvergne, H. Bouas-Laurent, F. Lahmani, J. Sepiol, *J. Phys. Chem.* **1992**, *96*, 10616; d) J. P. Desvergne, M. Gotta, J. C. Soulignac, J. Laurent, H. Bouas-Laurent, *Tetrahedron Lett.* **1995**, *36*, 1259–1262; e) H. Bouas Laurent, A. Castellan, J.-P. Desvergne, R. Lapouyade, *Chem. Soc. Rev.* **2000**, *29*, 43–55; f) H. Bouas Laurent, A. Castellan, J.-P. Desvergne, R. Lapouyade, *Chem. Soc. Rev.* **2001**, *30*, 248–263.

[12] a) V. R. Sastri, R. Schulman, D. C. Roberts, *Macromolecules* **1982**, *15*, 939–947; b) M. Okada, Y. Takashima, A. Harada, *Macromolecules* **2004**, *37*, 7075–7077.

[13] For example, see: a) N. Ide, Y. Tsujii, T. Fukuda, T. Miyamoto, *Macromolecules* **1996**, *29*, 3851–3856; b) J. R. Jones, C. L. Liotta, D. M. Collard, D. A. Schiraldi, *Macromolecules* **2000**, *33*, 1640–1645; c) C. Bratschkov, *Eur. Polym. J.* **2001**, *37*, 1145–1149; d) Y. Zheng, M. Micic, S. V. Mello, M. Mabrouki, F. M. Andreopoulos, V. Konka, S. M. Pham, R. M. Leblanc, *Macromolecules* **2002**, *35*, 5228–5234; e) M. J. Mack, C. D. Eisenbach, *Mol. Cryst. Liq. Cryst.* **2005**, *431*, 97–102.

[14] Y. Takaguchi, Y. Yanagimoto, T. Tajima, K. Ohta, J. Motoyoshiya, H. Aoyama, *Chem. Lett.* **2002**, 1102–1103.

[15] a) M. Okada, A. Harada, *Org. Lett.* **2004**, *6*, 361–364; b) R. Eckel, C. Schäfer, R. Ros, D. Anselmetti, J. Mattay, *J. Am. Chem. Soc.* **2007**, *129*, 1488–1489.

[16] In the present paper's context the regiochemical course of the dimerization may be of importance. It should, therefore, be pointed out that *head/head* couplings can be the favored products if the monomers are pre-oriented appropriately.

[17] a) Y. Takaguchi, T. Tajima, Y. Yanagimoto, S. Tsuboi, K. Ohta, J. Motoyoshirya, H. Aoyama, *Org. Lett.* **2003**, *5*, 1677–1679; b) D.-Y. Wu, B. Chen, X.-G. Fu, L.-Z. Wu, L.-P. Zhang, C.-H. Tung, *Org. Lett.* **2003**, *5*, 1075–1077.

[18] The main "side product" was of course the dimer of parent anthracene. It is reasonable to assume that, in addition, not only 3:1 but also 2:1 and 1:1 adducts between **3** and anthracene were formed. Furthermore, an intramolecular self-dimerization of two of the three anthracene units of **3** can be envisioned.

[19] Preliminary grazing incidence IR spectroscopical investigations show that these lines (1454 and 1474 cm^{-1}) can also be observed on freshly polymerized films while still being at the interface: G. Brezesinski, K. Wagner, H. Möhwald, C. Münzenberg, A. D. Schlüter, in preparation.

[20] H.-D. Becker, V. Langer *J. Org. Chem.* **1993**, *58*, 4703–4708.

[21] Considering the flexibility of monomers with pendent anthracene units it is not clear whether in a compressed monolayer these units are pointing upwards giving rise to *hh* dimers or are pointing more or less towards neighboring monomers leading to *ht* dimers.

[22] These signals were not detected after photochemical treatment of a monolayer of 10-thiodecyl-2-anthryl ether on gold, which also gave anthracene dimers: a) M. A. Fox, M. D. Wooten, *Langmuir* **1997**, *13*, 7099–7105, which is in contradiction to preliminary GI-IR experiments on phototreated monolayers of **16b** carried out in the laboratory of Prof. H. Möhwald, MPI-KG, Potsdam-Golm, which clearly show signals at 1454 and 1474 cm^{-1} (G. Brezesinski, unpublished results). A possible explanation may be a different orientation of the dimers relative to the surface. According to selection rules for surface IR spectroscopy, a mode is active if its dipole moment projects at a non-zero angle from the surface normal: b) J. Fan, M. Trenary, *Langmuir* **1994**, *10*, 3649–3657; c) S.-C. Chang, I. Chao, Y.-T. Tao, *J. Am. Chem. Soc.* **1994**, *116*, 6792–6805.

[23] G. Deng, T. Sakaki, Y. Kawahara, S. Shinkai, *Tetrahedron Lett.* **1992**, *33*, 2163–2166.

[24] In the all-trans conformation the height of **16a** was estimated as 24 Å.

[25] J. F. Moulder, W. F. Stickle, P. E. Sobol, K. D. Bomben, *Handbook of X-ray Photoelectron Spectroscopy. A Reference Book of Standard Spectra for the Identification and Interpretation of XPS Data*, **1992**, Perkin–Elmer Corporation.

[26] G. Beamson and D. Briggs, *High Resolution XPS of Organic Polymers: The Scienta ESCA 300 Database*, Wiley, Chichester.

[27] a) A. Rossi, B. Elsener, *Surf. Interface Anal.* **1992**, *18*, 499–504; b) N. P. Huang, R. Michel, J. Vörös, M. Textor, R. Hofer, A. Rossi, D. L. Elbert, J. A. Hubbell, N. D. Spencer, *Langmuir* **2001**, *17*, 489–498.

[28] M. A. Fox, M. D. Wooten, *Langmuir* **1997**, *13*, 7099–7105.

[29] a) D. Day, H. Ringsdorf, *J. Polym. Sci. Polym. Lett. Ed.* **1978**, *16*, 205–210; b) D. Day, J. B. Lando, *Macromolecules* **1980**, *13*, 1478–1483; c) H. Bader, K. Dorn, B. Hupfer, H. Ringsdorf, *Adv. Polym. Sci.* **1985**, *64*, 1–62; d) D. Lefevre, F. Porteu, P. Balog, M. Roulliay, G. Zalczer, S. Palacin, *Langmuir* **1993**, *9*, 150–161; e) S. Palacin, F. Porteu, A. Ruaunde-Feixier, *Thin Films* **1995**, *20*, 69–82.

[30] A. Ulman, *An Introduction to Ultrathin Organic Films From Langmuir–Blodgett to Self-Assembly*, Academic Press, San Diego, **1991**.

[31] V. V. Martin, L. Lex, J. F. W. Keana, *Org. Prep. Proc. Intl.* **1995**, *27*, 117–120.

[32] M. Segura, F. Sansone, A. Casnati, R. Ungaro, *Synthesis* **2001**, 2105–2112.

[33] M. A. O. Oar, J. M Serin, W. R. Dichtel, J. M. J. Fréchet, *Chem. Mater.* **2005**, *17*, 2267–2275.

[34] Y. Zhao, E.-H. Ryu, *J. Org. Chem.* **2005**, *70*, 7585–7591.

[35] a) P. Kenis, O. Noordman, H. Schönherr, E. Kerver, B. Snellink-Ruëll, G. van Hummel, S. Harkema, C. van der Vorst, J. Hare, S. Picken, J. Engbersen, N. van Hulst, G. Vancso, D. Reinhoudt, *Chem. Eur. J.* **1998**, *4*, 1225–1234; b) F. Sansone, M. Dudic, G. Donofrio, C. Rivetti, L. Baldini, A. Casnati, S. Cellai, R. Ungano, *J. Am. Chem. Soc.* **2006**, *128*, 14528–14536.

[36] H. O. House, J. A. Hrabie, D. VanDerveer, *J. Org. Chem.* **1986**, *51*, 921–929.

[37] W. H. Pirkle, J. M. Finn *J. Org. Chem.* **1983**, *48*, 2779–2780.

Received: March 14, 2008
Revised: July 31, 2008
Published online: October 22, 2008

